Proceedings of the Pakistan Academy of Sciences: A Physical and Computational Sciences 62(2): 107-121 (2025)

ISSN (Print): 2518-4245; ISSN (Online): 2518-4253
http://doi.org/10.53560/PPASA(62-2)687

Pakistan Academy of Sciences

Research Article

Lithofacies and Grain-size Analysis of the Oligocene Nari Formation, Benir Anticline, Southern Indus Basin, Pakistan: Evidence of a Marine-to-Continental Depositional Shift

Asghar A.A.D. Hakro[1], Aijaz Ali Halepoto[1*], Surriya Bibi Ahmedani[1,2], Abdul Samad Bhutto[3], and Abdul Shakoor Mastoi[1]

[1]Centre for Pure and Applied Geology, Faculty of Natural Sciences, University of Sindh, Jamshoro, Pakistan
[2]Government Zubeda Girls College, Hyderabad, College Education Department, Government of Sindh, Pakistan
[3]Pakistan Petroleum Limited, PIDC House, Dr. Ziauddin Ahmed Road, Civil Lines, Karachi, Sindh, Pakistan

Abstract: In the Southern Indus Basin, Pakistan, the Nari Formation of Oligocene age represents an important stratigraphic unit that preserves a classical regressive depositional sequence, recording a significant transition from marine to continental environments. This study analyzes the lithofacies and grain-size parameters of the Nari Formation from the Benir anticline section, Southern Indus Basin, to interpret its depositional environments. A 65 m thick stratigraphic section was measured and divided into non-clastic and clastic lithofacies groups. Non-clastic lithofacies group observed in the lower part of the Nari Formation and consists of compacted limestone, coquinoidal limestone and arenaceous limestone lithofacies, indicating deeper outer-ramp to near-shore depositional environments. The clastic lithofacies group was identified in the upper part, which consists of calcareous sandstone, variegated and gypsiferous shale, lateritic sandstone and friable sandstone lithofacies, suggesting continental fluvial depositional conditions. Shale-bearing lithofacies were identified in the middle part of the Nari Formation, reflect evaporitic and oxidizing continental settings. Grain-size analysis of eleven samples from friable sandstone facies supports a river-dominated origin. The vertical transition from marine to continental facies in the Nari Formation reflects a significant depositional shift, documenting a regressive sequence from marine ramp to fluvial settings. This study contributes to the broader understanding of the stratigraphic evolution of the Southern Indus Basin in relation to Oligocene regional tectonic background.

Keywords: Lithofacies, Grain-size Analysis, Depositional Environment, Oligocene, Nari Formation.

1. INTRODUCTION

The analysis of lithofacies has long been an essential tool in deciphering sedimentary processes and depositional environments [1-4]. By examining sedimentary structures, texture, mineral composition and fossils content, lithofacies analysis enables the interpretation of various depositional systems such as fluvial, deltaic and shallow marine environments [4-6]. Lithofacies analysis is generally supplemented with grain-size analysis, petrography, geochemistry and advanced technologies, such as scanning electron microscope (SEM), X-ray diffraction (XRD) and X-Ray Computed Tomography [2, 6-9]. Among these, the grain-size analysis is widely used to determine sediment transport mechanisms, energy conditions and depositional settings [6, 10-12]. The Oligocene is a crucial epoch in the geological history of the Indus Basin, marked by significant tectonic and

Received: March 2025; Revised: May 2025; Accepted: June 2025
* Corresponding Author: Aijaz Ali Halepoto <aijaz.halepoto@usindh.edu.pk>

depositional changes [12-14]. These changes were driven by progressive continent-continent collision of the Indian and Eurasian Plates [13-17]. The Nari Formation is a key stratigraphic unit that preserved exceptional record of these tectonic and depositional changes. Therefore, understanding its lithofacies characters and depositional environment is vital for reconstructing the Oligocene geological history of the region. The Benir anticline, a doubly plunging, north-south trending structure located in the southeastern Kirthar Fold Belt, offers well-preserved exposures of the Nari Formation. Previously, Nari Formation was studied in terms of provenance [18, 19], depositional environment [10, 12, 20, 21] and diagenesis [22-24]. During previous studies, textural, mineralogical and geochemical attributes of the Nari Formation have been explored from different exposed sections in the Southern Indus Basin. However, a systematic lithofacies record capturing the full spectrum of depositional environments and their stratigraphic transitions within the Nari Formation is not yet clearly understood. The present study aims to bridge this research gap by conducting its comprehensive lithofacies and grain-size analysis from the Benir anticline section, Southern Indus Basin. The results of this study will not only enhance our understanding of the sequential changes in the depositional environment during the Oligocene in the study area, but also contribute to understanding the depositional environment shift from marine to continental settings in response to plate collision along the western margin of the Indus Basin, Pakistan.

2. GEOLOGICAL BACKGROUND

The Indus Basin is situated in the northwestern part of the Indian Plate [17, 25]. It is bordered by the Indian Shield in the east, the Himalayas in the north, the Suleiman and Kirthar ranges in the west and the Arabian Sea in the south [26-31]. The western part of the Indus Basin became the foreland basin in response to continent-continent collision between the Indian and Eurasian Plates during the Cenozoic [12, 16, 17, 29]. The Indus Basin is divided into upper and lower parts by the Precambrian Shield elements, exposed in the Sargodha High [25, 26]. The Lower Indus Basin is further divided into central and southern parts by the "Sukkur Rift Zone" [26, 30]. The Southern Indus Basin comprises four most dominant tectonic units, which are the Precambrian Indian Shield ("Nagarparkar Igneous Complex (NIC)", the Indus Platform, the Kirthar Foredeep and the Kirthar Fold Belt [17, 27, 31, 32]. The NIC is composed of an-orogenic (A-type), igneous (I-type) granite, low-grade metamorphic rocks, acidic and basic dikes and rhyolite plugs [33, 34]. The NIC is part of the basement of the Southern Indus Basin, which is overlain by Mesozoic and Cenozoic rocks [17, 25, 26].

The Indus Platform is a gently west-dipping platform that consists of Mesozoic sedimentary rocks cut by Late Cretaceous normal faults [17, 26, 35]. The Mesozoic rocks of the Indus Platform are unconformably overlain by generally undeformed Tertiary rocks [25, 36, 37]. The Kirthar Foredeep is a down-warped segment of the Southern Indus Basin due to lithospheric flexure in front of the growing Kirthar and Suleiman ranges [17, 26, 38]. It consists of thick post-Eocene sedimentary rocks, particularly the Neogene Molasses of the Manchar Formation. The western part of the Southern Indus Basin is structurally deformed due to its oblique collision with the Afghan Block along the Ornach-Nal Fault [39-41]. This deformed part is called the "Kirthar Fold Belt" [17, 26, 31]. The western part of the Kirthar Fold Belt consists of exposed Bela Ophiolites and Mesozoic sedimentary rocks, whereas Cenozoic rocks are predominantly exposed in its eastern part [28, 42, 43] (Table 1). The present study area is located in the southeastern part of the Kirthar Fold Belt (Figure 1).

3. MATERIALS AND METHODOLOGY

Detailed geological fieldwork of the Nari Formation was carried-out from the Benir anticline (Latitude 25°27'18.50" N, Longitude 67°36'51.12" E). The lower contact of the Nari Formation is not exposed in the study area; therefore, measurement was started from core of the Benir anticline (Figure 2(a)). Individual lithofacies were identified and their thickness in the stratigraphic section were measured with help of measuring tape. The total measured thickness of the Nari Formation in study area is 65 m (Figure 2(b)). All lithofacies were described based on their outcrop and lithological attributes, such as lithology, texture, fossils and sedimentary structure. During the measurement of the stratigraphic section, thirty-five lithological strata were identified and sampled, which included 16 limestone, 11 sandstone, 4 shale and 4 lateritic

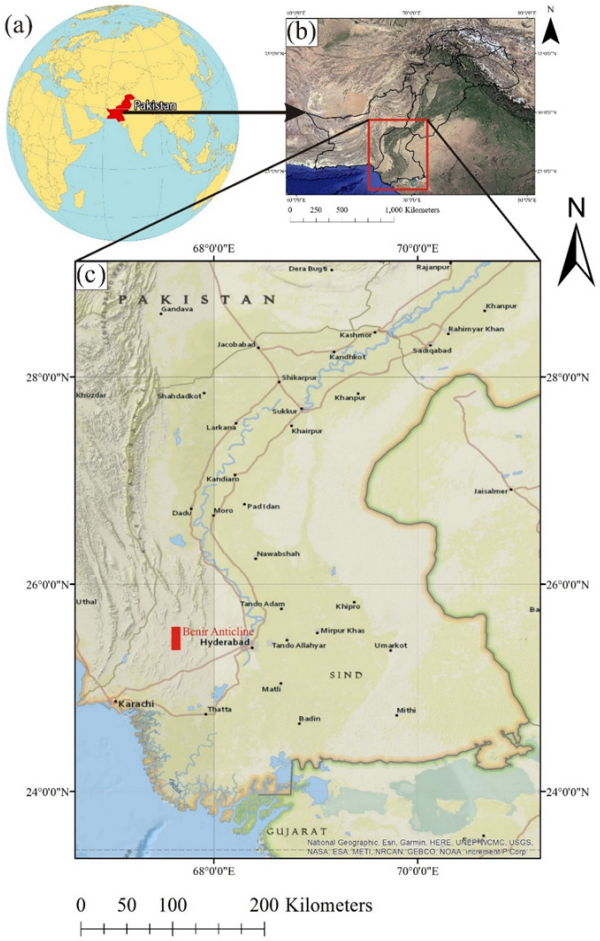

Fig. 1: Location map of the Benir anticline (Image Source-National Geo-graphic, Esri, Garmin, HERE, UNEPWCMC, USGS, NASA, ESA, METI, NRCAN, GEBCO, NOAA, increment P Corp. & gisgeography.com).

or oxidized sandstone. These strata were broadly classified into two lithofacies groups, i.e., non-clastic and clastic lithofacies groups. The non-clastic lithofacies group is further divided into three distinct lithofacies based on their lithology and relative abundance of fossils contents. The clastic lithofacies group is further classified into four lithofacies based on their lithological aspects. From the thirty-five samples, 11 loose and friable sandstone were selected for grain-size analysis (Figure 2(b)). Most of the loose and friable sandstone

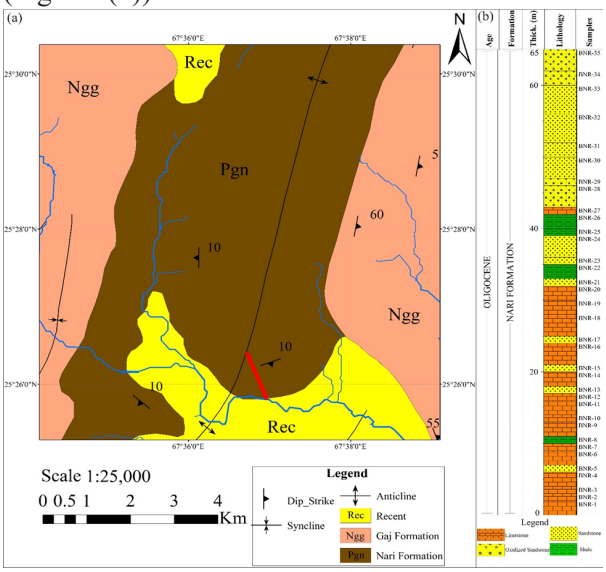

Fig. 2: (a) Geological map of the Benir anticline, showing the location of the measured section marked with a bold red line (after [17, 42]). (b) Lithological column of the measured section indicating formation thickness and sample numbers.

Table 1. Exposed stratigraphy of the Southern Indus Basin (after [28, 42]).

Age	Formation	Lithology
Pleistocene	Dada Conglomerate	Conglomerate, Boulders and Pebbles
Neogene	Manchar Formation	Sandstone, Shale and Conglomerate
Miocene	Gaj Formation	Sandstone, Shale, Limestone
Oligocene	Nari Formation	Limestone, Shale and Sandstone
Eocene	Kirthar Formation	Limestone
	Tiyon formation	Limestone, Shale, Marl
	Laki Formation	Limestone, Shale, and Sandstone
Paleocene	Lakhra Formation	Limestone, Shale and Sandstone
	Bara Formation	Sandstone, Claystone and Shale
	Khadro Formation	Sandstone, Shale and Limestone
	Khaskheli Basalt	Basalt
Cretaceous	Pab Sandstone	Sandstone
	Fort Munro Formation	Limestone and Marl

is observed in the upper part of the measured section, which lacked depositional features, such as bed geometry, sedimentary structures, or fossils contents. Therefore, their samples were analyzed in terms of their grain-size distribution. The standard sieving method was adopted to process, classify and analyze different groups of grain-sizes in the studied samples [10, 44-46]. The grain-sizes in millimeters, obtained through sieve analysis were converted to "phi (φ)" scale, which is a logarithmic scale to base 2 [6, 47]. Cumulative frequency curves for each analyzed sample were drawn from the weight percentage of each grain size in the sample. Different grain-size parameters, such as mean, median, standard deviation, skewness, kurtosis etc., of each sample were calculated from cumulative frequency curves. Different bivariate interpretation diagrams were prepared by plotting grain-size parameters against each other to understand the textural character, transportation mechanism and depositional environment of the loose and friable sandstone of the Nari Formation [6, 12, 45].

4. RESULTS

4.1. Lithofacies Analysis

The lower contact of the Nari Formation is not exposed in the Benir anticline section, whereas it has either a sharp upper contact with the Miocene Gaj Formation, or its upper contact is covered with the Holocene deposits. The Nari Formation exhibits diverse and distinct patterns of lithologies from base to top, which are broadly classified into non-clastic and clastic lithofacies groups (Figure 2).

4.1.1. Non-clastic Lithofacies Group

The lithofacies of this group were identified in the lower part of the Nari Formation in the study area. These lithofacies are dominantly composed of limestone and are further classified into three lithofacies types based on lithological features and the relative abundance of fossils contents.

(a) Compacted Limestone Facies

These lithofacies were identified in the lower part and consists of eight strata (BNR-1, 3, 6, 10, 11, 12, 14 and 27) with a cumulative thickness of 12 m. These are characterized by orange-yellow to creamy yellow, well compacted and jointed limestone, fossiliferous, but it contains rare larger benthic foraminifera (Figure 3(a)). These lithofacies are dominantly composed of fine-grained calcareous and bioclastic material along with mega-fossils of gastropods, echinoids and bivalves. These contains fibrous sparry calcite, which forms flower-shaped structures within limestone (Figures 3(b), 5(b)). The texture of these lithofacies resembles with the mudstone-wackstone, because they consist of higher fine-grained calcareous content than larger bioclasts. The dominancy of fine-grained calcareous material indicate deposition under low-energy marine environment, below storm weather wave-base [48, 49]. The gastropods, echinoids and bivalves are generally tend to live in shallow coastal areas to deep marine environments, around the world [50-52]. Therefore, these lithofacies of the Nari Formation are interpreted to be deposited in the open-marine, distal part of the outer-ramp, under low-energy depositional environment.

(b) Coquinoidal Limestone Facies

These lithofacies were also identified in the lower part of the Nari Formation in the studied section. These consists of four strata (BNR-2, 4, 7 and 9) with a cumulative thickness of 6 m. They are characterized by orange-yellow well compacted and in places, moderately compacted limestone. These lithofacies are dominantly composed of tests of larger benthic foraminifera, particularly *Discocyclina* and *Nummulites,* and broken shelly fragments. The abundance of foraminiferal tests gives the limestone a distinctive biogenic character. The bioclasts are generally poor to moderately sorted and aligned horizontally to the bedding planes (Figure 3(c-e)). The texture of thess lithofacies resembles with the wackstone packstone, because it consists of lower mud matrix content than bioclasts. *Discocyclina* is reported to occur in the outer-ramp, low-energy and under lower photic zone depositional settings [53-56] The abundance of *Discocyclina* with *Nummulites* has been reported from the middle to outer ramp of the Eocene carbonates [57-59]. Therefore, Coquinoidal limestone lithofacies of the Nari Formation are interpreted to have been deposited in the middle to outer ramp depositional environment. Alternation of coquinoidal and compacted limestone facies suggest middle to distal part of outer-ramp depositional environment during deposition of lower part of the Nari Formation in study area.

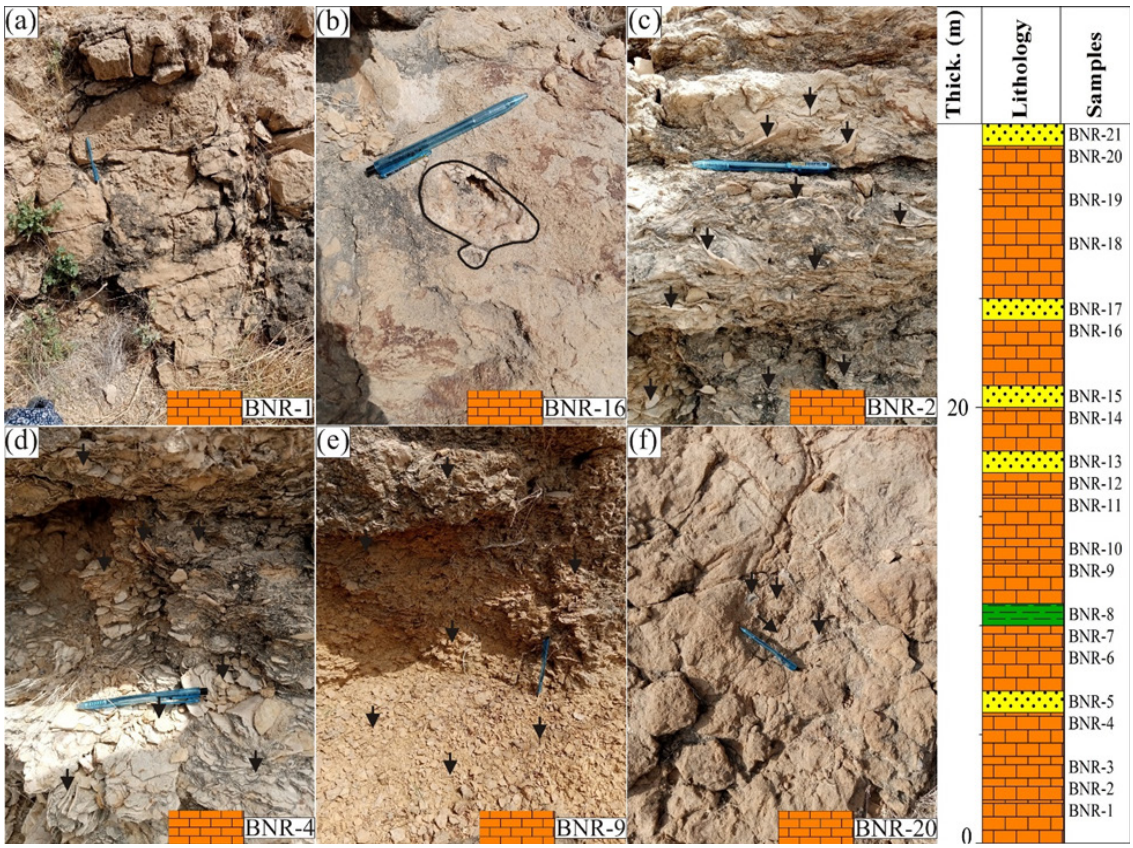

Fig. 3: Non-clastic lithofacies of the Nari Formation in the studied section and their respective positions in the lithological column. (a, b) Compacted limestone facies. The black polygon in (b) outlines sparry calcite. (c, d) Coquinoidal limestone facies dominantly composed of bioclasts of *Discocyclina*. (e) Coquinoidal limestone facies dominantly composed of *Discocyclina* and *Nummulites* tests. (f) Arenaceous limestone facies.

(c) Arenaceous Limestone Facies

These lithofacies were identified in the middle part of the Nari Formation in the study area. These consists of four strata (BNR-16 and 18-20) with a cumulative thickness of 10 m. These are reddish-gray, well-compacted limestone facies, which consist of a significant proportion of sand. These lithofacies contain worm-burrows, fossils of plecypods and bivalves (Figure 3(f)). The presence of a significant proportion of medium-grained sand in these lithofacies suggest enhanced sediment supply from the continent [58, 60]. The presence of worm-burrows associated with plecypods and bivalves is an indication of a coastal environment [51, 61]. Therefore, arenaceous limestone facies of the Nari Formation were deposited in the near-shore depositional environment. As these lithofacies overlie the middle to outer-ramp deposited-facies, hence indicate progressively decreasing sea-levels during the deposition of the Nari Formation in the study area.

4.1.2. Clastic Lithofacies Group

The lithofacies of this group were identified in the middle to upper part of the Nari Formation in the study area (Figure 4(a)). These lithofacies are dominantly composed of sandstone and shale. Lithofacies of this group are further classified into four lithofacies types based on differences in lithological features.

(a) Calcareous Sandstone Facies

These lithofacies were identified in the middle part of the Nari Formation and it overlies the arenaceous limestone facies. These consists of six strata (BNR-13, 15, 17, 21, 23 and 24) with a cumulative thickness of 8 m. These are light-yellow to grayish-yellow, moderately compacted to friable sandstone facies, which consist of calcareous material, possibly as cementing material. No primary sedimentary structures and fossils were identified in these strata (Figures 4(b, d, e)). The

depositional environment of these lithofacies could not be precisely determined due to lack of primary sedimentary structures and fossil contents. Therefore, friable samples of these lithofacies were studied through grain-size analysis.

(b) Variegated and Gypsiferous Shale Facies

Four strata of shale were identified, one in the basal (BNR-8) and three in the middle part (BNR-22, 25 and 26) of the Nari Formation in the studied section. These lithofacies have a cumulative thickness of 6 m, and exhibit diverse color ranges (Figures 4(c, f)). BNR-22 and 25 are variegated and contain abundant gypsum veins (Figure 4(f)). BNR-26 is oxidized, dark red to reddish-brown and it does not contain any evaporitic mineral (Figure 5(a)). Shale deposits in low-energy depositional settings of floodplain, lake, lagoon or deep-marine environments, where fine sediments settle out of slow-moving or quite water [62-64]. Gypsum often forms in arid or semi-arid regions due to evaporation of sea-water [65, 66]. The oxidized nature of shale also suggests the continental oxidizing environment. This evidence suggests, these lithofacies of the Nari Formation were deposited in a continental shallow-water evaporative lagoon.

(c) Lateritic Sandstone Facies

These lithofacies were identified in the upper part of the Nari Formation in the studied section. These consists of four strata (BNR-28, 29, 34, and 35) with a cumulative thickness of 9 m. These are pinkish-brown, light pink and brownish-red, moderately compacted to friable, highly oxidized and jointed sandstone (Figures 5(c, d)). No primary sedimentary structures were identified in these strata, but their lithological character suggests oxidizing continental deposition or prolonged exposure of sediment surface to oxygen-rich environmental conditions. Its stratum BNR-28

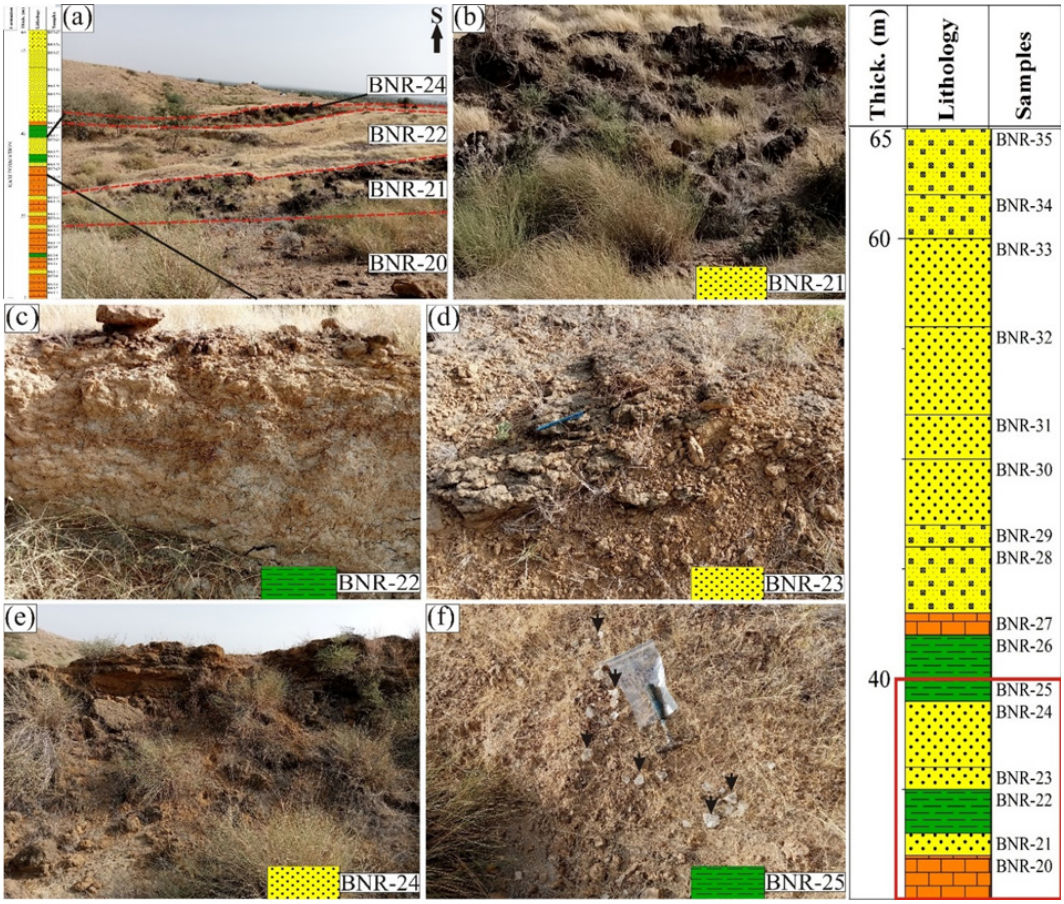

Fig. 4: Clastic lithofacies of the Nari Formation in the studied section and their respective positions in the lithological column shown within red rectangle. Field photograph (a) showing lithofacies stacking pattern. (b) Calcareous sandstone facies. (c) Gypsiferous shale facies. (d, e) Calcareous sandstone facies. (f) Variegated and gypsiferous shale facies.

overlies the compacted limestone facies stratum 27, indicating sharp transition from deeper distal outer-ramp environment to continental environmental conditions. Grain-size analysis of friable samples of these lithofacies has been carried out to support the lithofacies interpretation.

(d) Friable Sandstone Facies

These were identified in the upper part of the Nari Formation and consists of four strata (BNR-30-33) with a cumulative thickness of 13 m. These are light gray to reddish-gray, friable to loose and massive sandstone (Figures 5(e, f)). No primary sedimentary structures were identified in these facies; hence, their depositional environment could not be determined. Therefore, friable samples of these lithofacies were studied through grain-size analysis to understand their depositional environment.

4.2. Grain-size Analysis

Grain-size analysis of loose and friable sandstone involves the systematic measurement and statistical characterization of grain diameters to determine their textural properties. The grain-size distribution provides critical insights into depositional environment and transport mechanisms [6, 12]. Well-sorted sandstones with narrow grain-size distributions typically indicate uniform depositional conditions, such as Aeolian or mature beach systems, while poorly sorted samples suggest rapid deposition or limited transport distances. The presence of bimodal or polymodal distributions may indicate mixing of different sediment sources or multiple depositional episodes [12, 45]. Statistical parameters calculated from grain-size analysis of the Nari Formation during the present study are presented in Table 2.

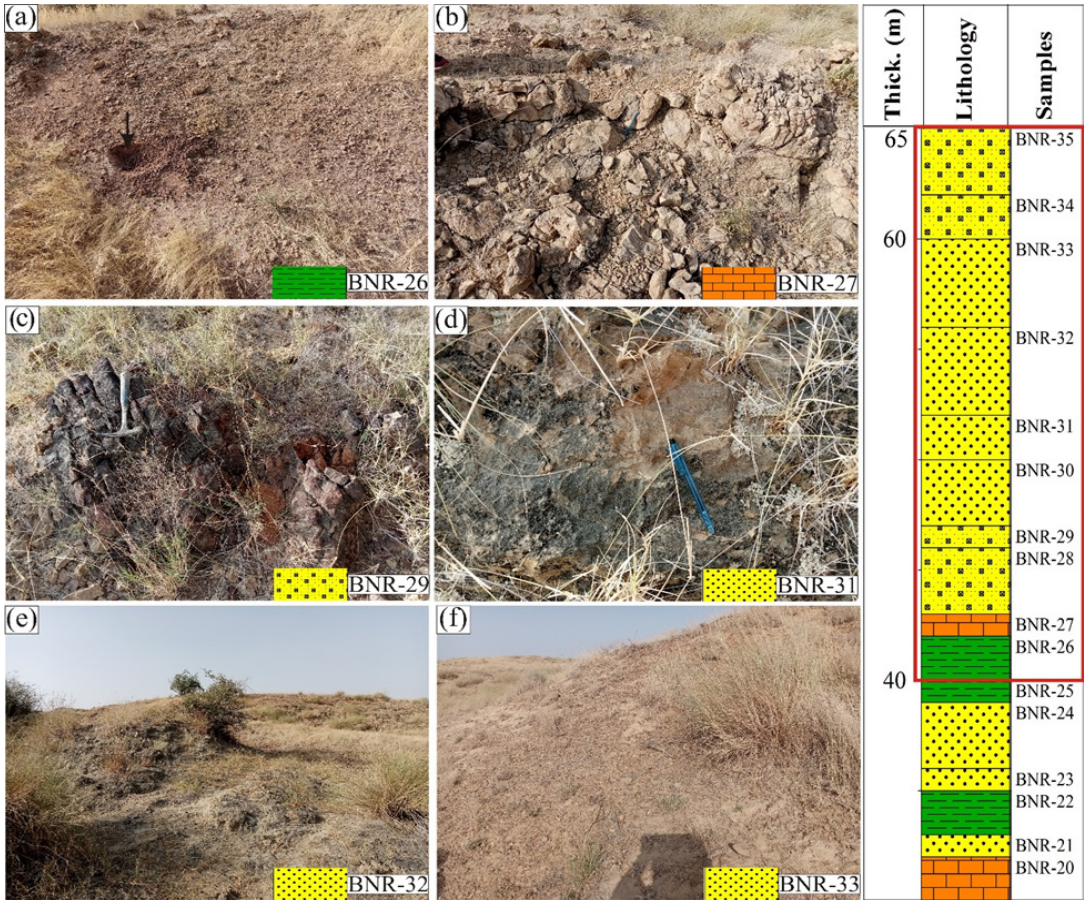

Fig. 5: Clastic lithofacies of the Nari Formation in the studied section and their respective positions in the lithological column shown within red rectangle. (a) Variegated and oxidized shale facies. (b) Compacted limestone facies. (c, d) Lateritic sandstone facies. (e, f) Friable sandstone facies.

Table 2. Grain-size parameters ("phi (φ)" unit) of the Nari Formation from Benir anticline.

S. No.	Sample	Mean	Median	Standard Deviation	Skewness	Kurtosis	C	M
1	BNR. 5	2.06	2.2	1.74	-0.21	1.33	846.75	217.64
2	BNR. 8	0.56	1	1.03	0.08	1.29	716.98	500.00
3	BNR.13	1.96	1.9	1.75	-0.13	0.53	812.25	267.94
4	BNR. 17	0.96	1.8	1.18	-0.15	1.49	687.77	287.17
5	BNR. 25	0.86	0.9	1.28	-0.05	0.65	737.13	535.89
6	BNR. 26	0.23	1.5	1.26	0.01	0.83	747.42	353.55
7	BNR. 28	1.93	1.8	1.68	-0.01	1.54	870.55	287.17
8	BNR. 30	1.7	1.6	1.32	0.08	1.36	933.03	329.88
9	BNR. 31	1.43	1.4	1.15	0.04	1.7	870.55	378.93
10	BNR. 33	1.7	1.6	1.3	1.23	1.48	972.65	329.88
11	BNR. 34	1.9	1.8	1.81	-0.08	2.28	768.44	287.17

4.2.1. Mean

The mean grain size values suggest the relative size of clasts, where a 0 value of phi (φ) indicates coarse sand and 3 indicates very fine sand. The studied samples show mean grain size in the range of 0.23-2.06 φ (coarse to fine), with an overall average of 1.39 φ (Table 2) (Figures 6(a-c)). The average mean size of the studied samples indicates the medium-grained sand. Mean grain size reflects the average energy conditions during deposition, with finer grains indicating lower energy environments. The variations in the mean grain-size value indicate fluctuations in the depositional energy level [6, 11, 63].

4.2.2. Median

It is the central grain size of a studied sample, for which half of the grains in that sample are larger than it, and half are smaller. The median grain-size value gives a good approximation of grain-size of studied strata. The studied samples show median size value in the range of 0.9-2.2 φ, with an average median size of 1.6 φ. This average median value indicates presence of medium-grained sand in the studied samples [6, 12, 45].

4.2.3. Standard Deviation (Sorting)

This statistical parameter determines level of sorting of the sediments [63]. The standard deviation value of 0 is taken as very well sorted sediments and any positive integer more than 2 is considered as very poorly sorted [63]. Sorting in turn is used to understand the hydrodynamic conditions or degree of reworking in the depositional system. Sorting is determined by transport processes, deposition and post-depositional processes such as winnowing or reworking [62, 63]. The standard deviation values of the Nari Formation in the Benir anticline section range between 1.03 to 1.81 φ, having an average of 1.40 φ. The standard deviation range of studied sediments indicate poor sorting (Figure 6(b)). This suggests that analyzed sediments were deposited in low-energy conditions and, therefore, didn't experience significant reworking during their deposition.

4.2.4. Skewness

The skewness is another statistical grain-size parameter of sorting, which indicate symmetry of grain size distribution in the studied samples. Measured skewness values of the studied samples of the Nari Formation ranges from -0.21 to 1.23 φ, having average of 0.07 φ. The skewness range of the studied sediments shows coarse-skewed to near symmetrical, while average skewness represents near symmetrical nature of sandstone of the Nari Formation (Figures 6(a, d)). The coarse-skewed to symmetrical nature of the sediments suggest the presence of poorly-sorted clasts, which were deposited in medium to low-energy conditions [12, 67-70].

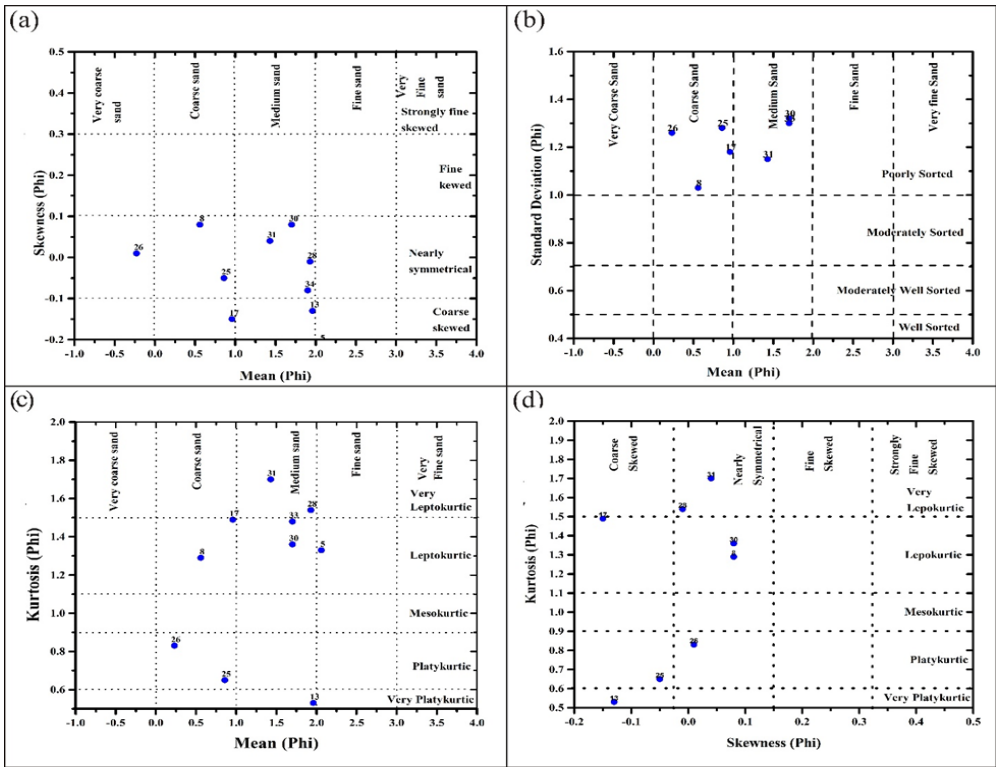

Fig. 6: Plots of grain-size parameters of the Nari Formation. (a) Mean versus skewness. (b) Mean versus standard deviation. (c) Mean versus kurtosis. (d) Skewness versus kurtosis.

4.2.5. Kurtosis

The kurtosis range of the Nari Formation in the studied section ranges from 0.53 to 1.50 φ with an average of 2.28 φ. Most samples of the Nari Formation show leptokurtic to very leptokurtic nature, while some samples indicate very platykurtic and platykurtic (Figures 6(c, d)). The kurtosis pattern indicates medium to low-energy depositional conditions during the deposition of the Nari Formation in the study area [12, 45].

4.2.6. Bivariate Statistical Diagrams

The bivariate statistical diagrams of grain-size distribution in the sedimentary rocks are valuable to diagnose the energy of the depositional medium as well as their depositional environment [44, 45, 67-70]. The median diameter plotted against standard deviation and mean diameter against skewness of analyzed sediments to distinguish between fluvial (river), shallow-marine (wave-dominated) and deep water (quiet water) deposition [12, 45, 67]. All analyzed samples of the Nari Formation from the Benir anticline fall in the "River" field of the "median versus standard deviation" diagram (Figure 7(a)). All analyzed samples also occupy the "River" field in the "mean versus skewness" diagram (Figure 7(b)). Therefore, these diagrams suggest that analyzed sediments of the Nari Formation were deposited in a fluvial (river-dominated) depositional environment.

4.2.7. Passega Diagram (CM Plot)

The CM plot (Passega diagram) was proposed by Passega [68] to identify sediment transport and depositional processes. These diagrams illustrate the correlation between 1% or one percentile (C) on the frequency curve of each sample and the median grain-size (M). Both these variables are first converted from φ (phi) in to µm and then M is plotted on the x-axis and C is plotted on the y-axis (Table 2). All the analyzed samples fall on 2 field between 1 and 3 fields on the CM plot diagram for transporting mechanism (Figure 7(c)). This indicates that analyzed sediments of the Nari Formation were transported through a rolling and suspension mechanism. All the studied samples fall between 4 and 5 fields on the CM plot diagram for depositional mechanism (Figure 7(d)), indicating deposition in fluvial conditions [6, 12, 45].

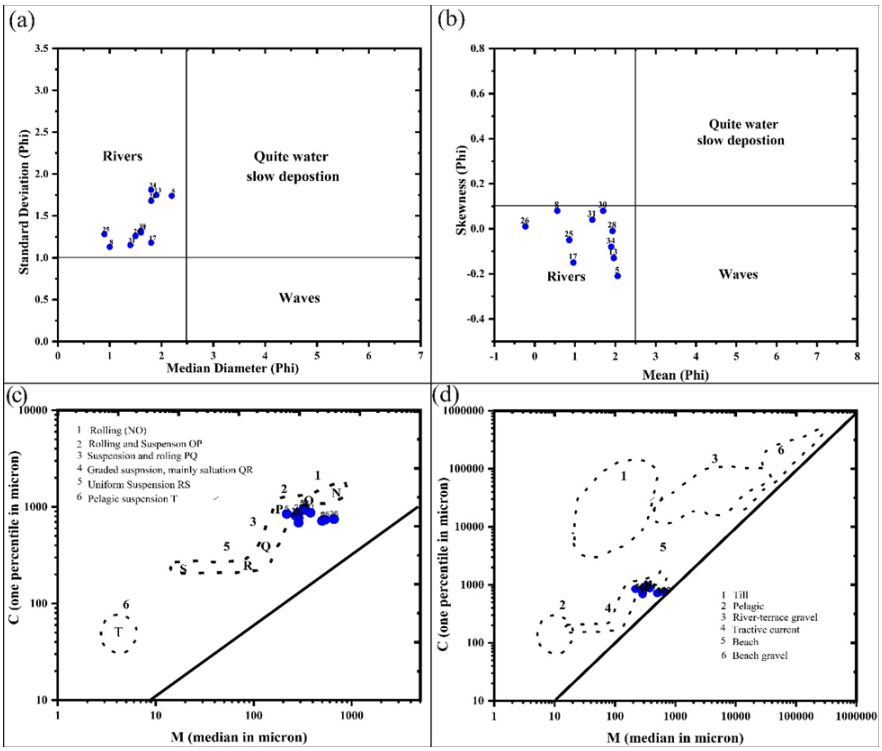

Fig. 7: (a) Median diameter versus standard deviation. (b) Mean diameter versus skewness. (c) Transportation mechanism. (d) Depositional mechanism of analyzed sediments of the Nari Formation, Benir anticline, Southern Indus Basin, Pakistan.

5. DISCUSSION

The lithofacies and grain-size analysis of the Nari Formation in the Benir anticline revealed a fascinating record of marine to continental depositional shift during the Oligocene in the Southern Indus Basin. The systematic vertical succession of lithofacies, which could be correlated with other prominent sections of the Nari Formation [21], demonstrates a clear regressive sequence that documents the progressive retreat of marine conditions and the establishment of continental depositional systems.

5.1. Marine Depositional Phase: Outer Ramp to Near Shore Settings

The lower part of the Nari Formation preserves evidence of initial marine deposition under outer-ramp settings. The compacted limestone facies, characterized by fine-grained calcareous material and mudstone-wackstone textures, indicate deposition in the distal outer-ramp environment below storm wave-base [48, 49]. This interpretation is also supported by the presence of marine fossils including gastropods, echinoids and bivalves, which collectively suggest low-energy, open-marine conditions [50-52]. The coquinoidal limestone facies, dominated by larger benthic foraminifera (*Discocyclina* and *Nummulites),* represents deposition in the middle to outer-ramp environment [53-56]. The abundance of these foraminifera, particularly *Discocyclina,* which thrives in outer-ramp, low-energy settings within the lower photic zone, confirms the marine origin of these sedimentary deposits [57-59]. The alternation between compacted limestone and coquinoidal limestone facies in the lower part provides crucial insights into the depositional dynamics of the marine ramp carbonate system and indicates frequent environmental changes from distal outer-ramp to middle to outer-ramp and vice versa. The transition to arenaceous limestone facies in the middle part of the Nari Formation marks a critical shift in the depositional system. The influx of significant proportions of sand, along with the presence of worm-burrows and shallow-marine fauna (plecypods and bivalves), indicates enhanced terrigenous input and shoaling conditions [21, 58, 60]. These facies represent deposition in the near-shore environment and provide the first clear evidence of marine regression and increasing

continental influence. The marine depositional phase of the Nari Formation in the Benir anticline section resembles that of the Hundi anticline section of the Nari Formation [21].

5.2. Continental Depositional Phase: Fluvial and Evaporitic Settings

The upper part of the Nari Formation documents a dramatic shift to continental depositional conditions, as evidenced by the clastic lithofacies group. The calcareous sandstone facies, lacking primary sedimentary structures and fossils, required grain-size analysis for environmental interpretation. The grain-size parameters consistently pointed to fluvial deposition, with bivariate diagrams placing all analyzed samples within the "River" field, confirming a fluvial depositional environment. The variegated and gypsiferous shale facies suggest deposition in evaporitic continental settings. The presence of abundant gypsum veins indicate arid to semi-arid climatic conditions with high evaporation rates, typical of continental evaporative lagoons or playa lake environments [62-64]. The oxidized nature of these shales, particularly the dark red to reddish-brown coloration, further supports continental oxidizing conditions and suggests periodic exposure to atmospheric oxygen [65, 66]. The lateritic sandstone facies represent the culmination of continental conditions, with its highly oxidized, pinkish-brown to brownish-red coloration indicating prolonged exposure to oxygen-rich environments. The sharp bedding plane between these facies and the underlying compacted limestone facies (stratum BNR-28 overlying stratum 27) dramatically illustrates the abrupt transition from middle to outer-ramp conditions to the continental environments, suggesting rapid regression or tectonic uplift. The continental depositional phase of the Nari Formation in the Benir anticline section is different than the Hundi anticline section of the Nari Formation [21]. It indicates that the continental depositional environments are highly unstable and their characteristics vary from place to place.

5.3. Energy Conditions and Transport Mechanisms

The grain-size analysis provides quantitative support for the environmental interpretations derived from lithofacies analysis. The mean grain-size values (0.23-2.06 φ) indicate predominantly medium-grained sand, suggesting moderate energy conditions during deposition. The poor sorting (standard deviation 1.03 to 1.81 φ) indicates limited reworking and transport, consistent with rapid deposition in relatively low-energy fluvial systems [6, 12, 45]. The skewness values (-0.21 to 1.23 φ) range from coarse-skewed to near-symmetrical, with an average near-symmetrical distribution. This pattern, combined with the kurtosis values showing leptokurtic to very leptokurtic distributions, confirms medium to low-energy depositional conditions [12, 67-70]. The Passega diagram analysis reveals that sediments were transported through rolling and suspension mechanisms and deposited under fluvial conditions, providing definitive evidence for the continental nature of the upper Nari Formation.

5.4. Regional Sequence Stratigraphic Significance

The marine to continental depositional transition documented in the Nari Formation reflects broader regional changes in the Southern Indus Basin during the Oligocene. This regression likely resulted from a combination of eustatic sea-level changes, regional tectonic uplift and increased sediment supply from the growing Himalayan orogen. The timing of this transition is consistent with the global Oligocene regression and the intensification of Himalayan uplift [4, 13, 17, 21]. The vertical succession of lithofacies in the Nari Formation represents a classic regressive sequence, documenting the progressive shoaling and eventual emergence of the depositional system [21]. The sharp bedding planes between marine limestone and continental sandstone facies suggest a rapid regression, possibly related to tectonic uplift or a significant drop in relative sea-level. This sequence provides valuable insights into the timing and mechanisms of basin evolution in the Southern Indus Basin and contributes to our understanding of the regional response to Himalayan orogeny.

6. CONCLUSIONS

The lithofacies and grain-size analysis of the Oligocene Nari Formation in the Benir anticline section has been carried out in order to shed light on its depositional environments and their shift from marine to continental conditions. The lower part of the Nari Formation consists of limestone-

dominated lithofacies, which were deposited in a deeper outer-ramp to near-shore depositional environment. Shale-dominated lithofacies were identified in the middle part of the Nari Formation, which are interpreted to have been deposited in the evaporitic and oxidizing settings. The upper part of the Nari Formation consists of sandstone-dominated lithofacies, which indicate deposition in continental conditions. Grain-size analysis of the sandstone facies suggest that these were deposited in fluvial or river-dominated depositional environments. Overall, the Nari Formation in the study area represents a well-preserved example of a regressive depositional sequence, documenting the progressive depositional regime shift from marine to continental conditions during the Oligocene. The marine to continental depositional shift was controlled by the Himalayan orogeny in the region.

7. ACKNOWLEDGMENTS

The authors are thankful to Prof. Dr. Rafique Ahmed Lashari, Director, Centre for Pure and Applied Geology, University of Sindh, Jamshoro, Pakistan, for providing transportation and other field-related facilities as well as permission of using sedimentological laboratories at the Centre for Pure and Applied Geology. We are thankful to the Wildlife Department, Government of Sindh for providing security and guiding personnel during the fieldwork. The authors are also thankful to Mr. Owais Khokhar, Aiza Preet Hakro and Muhammad Azeem for their assistance during fieldwork. We are thankful to Mr. Riaz Ali Shah, Field Driver, Centre for Pure and Applied Geology, University of Sindh, Jamshoro and Mr. Dad Muhammad Burfat for facilitating our fieldwork.

8. CONFLICT OF INTEREST

The authors declare no conflict of interest.

9. REFERENCES

1. S. Obaid, A.W. Qureshi, and I.A. Abbasi. Lithofacies, sand-bodies geometry and depositional setting of the Datta Formation in Surghar Range, North Pakistan. *SPE-PAPG Annual Technical Conference (28th - 29th November 2005)*, *Islamabad, Pakistan* (2005).
2. A.K. Srivastava and R.S. Mankar. Lithofacies architecture and depositional environment of Late Cretaceous Lameta Formation, Central India. *Arabian Journal of Geosciences* 8(1): 207-226 (2013).
3. A. Bilal, R. Yang, N. Lenhardt, Z. Han, and X. Luan. The Paleocene Hangu formation: A key to unlocking the mysteries of Paleo-Tethys tectonism. *Marine and Petroleum Geology* 157: 106508 (2023).
4. G. Métais, P.O. Antoine, S.R.H. Baqri, J.Y. Crochet, D. De Franceschi, L. Marivaux, and J.L. Welcomme. Lithofacies, depositional environments, regional biostratigraphy and age of the Chitarwata Formation in the Bugti Hills, Balochistan, Pakistan. *Journal of Asian Earth Sciences* 34(2): 154-167 (2009).
5. C. Wang, B. Zhang, Y. Lu, Z. Shu, Y. Lu, H. Bao, Z. Meng, and L. Chen. Lithofacies distribution characteristics and its controlling factors of shale in Wufeng Formation-Member 1 of Longmaxi Formation in the Jiaoshiba area. *Petroleum Research* 3(4): 306-319 (2018).
6. A.A.A.D. Hakro, A.A. Halepoto, M.S. Samtio, R.H. Rajper, A.S. Mastoi, R.A. Lashari, and M.A. Rahoo. The Comparative Depositional Heterogeneity of Manchhar Formation (Siwalik Group), Southern Indus Basin, Pakistan. *Journal of Mountain Area Research* 9: 1-15 (2024).
7. C. Klein and N.J. Beukes. Geochemistry and sedimentology of a facies transition from limestone to iron-formation deposition in the early Proterozoic Transvaal Supergroup, South Africa. *Economic Geology* 84(7): 1733-1774 (1989).
8. P. Wang, Z. Jiang, L. Yin, L. Chen, Z. Li, C. Zhang, T. Li, and P. Huang. Lithofacies classification and its effect on pore structure of the Cambrian marine shale in the Upper Yangtze Platform, South China: Evidence from FE-SEM and gas adsorption analysis. *Journal of Petroleum Science and Engineering* 156: 307-321 (2017).
9. J.E. Houghton, J. Behnsen, R.A. Duller, T.E. Nichols, and R.H. Worden. Particle size analysis: A comparison of laboratory-based techniques and their application to geoscience. *Sedimentary Geology* 464: 106607 (2024).
10. Q. Khokhar, A.A.A.D. Hakro, S.H. Solangi, I. Siddiqui, and S.A. Abbasi. Textural Evaluation of Nari Formation, Laki Range, Southern Indus Basin, Pakistan. *Sindh University Research Journal (Science Series)* 48(3): 633-638 (2016).
11. C. Baiyegunhi, K. Liu, and O. Gwavava. Grain size statistics and depositional pattern of the Ecca Group sandstones, Karoo Supergroup in the Eastern Cape Province, South Africa. *Open Geosciences* 9(1): 554-576 (2017).
12. A.A.A.D. Hakro, W. Xiao, A.S. Mastoi, Z. Yan, M.S. Samtio, and R.H. Rajper. Grain size analysis of the Oligocene Nari Formation sandstone in the Laki

Range, southern Indus Basin, Pakistan: Implications for depositional setting. *Geological Journal* 425: 5440-5451 (2021).

13. G. Zhuang, Y. Najman, S. Guillot, M. Roddaz, P.O. Antoine, G. Métais, A. Carter, L. Marivaux, and S.H. Solangi. Constraints on the collision and the pre-collision tectonic configuration between India and Asia from detrital geochronology , thermochronology , and geochemistry studies in the lower Indus basin , Pakistan. *Earth and Planetary Science Letters* 432: 363-373 (2015).
14. M. Qasim, O. Tayyab, L. Ding, J.I. Tanoli, Z.I. Bhatti, M. Umar, H. Khan, J. Ashraf, and I.A.K. Jadoon. Exhumation of the Higher Himalaya: Insights from Detrital Zircon U–Pb Ages of the Oligocene–Miocene Chitarwatta Formation, Sulaiman Fold–Thrust Belt, Pakistan. *Applied Sciences* 13(6): 3418 (2023).
15. L. Ding, M. Qasim, I.A.K. Jadoon, M.A. Khan, Q. Xu, F. Cai, H. Wang, U. Baral, and Y. Yue. The India-Asia collision in north Pakistan: Insight from the U–Pb detrital zircon provenance of Cenozoic foreland basin. *Earth and Planetary Science Letters* 455: 49-61 (2016).
16. A.A. Halepoto, M.H. Agheem, A.A.A.D. Hakro, S. Ahmed, and S.B. Ahmedani. Geometry and Kinematics of the Gentle to Open Fault-propagation Fold having Four-way Dip Enclosure: Outcrop and Lineament Analysis of the Rois Anticline, Southern Kirthar Fold Belt, Pakistan. *Journal of Himalayan Earth Sciences* 58(1): 88-106 (2025).
17. A.A. Halepoto, M.H. Agheem, A.A.A.D. Hakro, S. Ahmed, and S.B. Ahmedani. Lateral Strike-slip Deformation and Possible Transition of Extensional Faults to Strike-slip Faults in the Foreland Fold Belt: A Regional to Outcrop Tectonic Synthesis of the Southern Kirthar Fold Belt, NW Indian Plate, Pakistan. *Journal of Asian Earth Sciences* 291: 106678 (2025).
18. Z. Ahmed, A.S. Khan, and B. Ahmed. Sandstone Composition and Provenance of the Nari Formation, Central Kirthar Fold, Pakistan. *Pakistan Journal of Geology* 4(2): 90-96 (2020).
19. A.A.A.D. Hakro, M.S. Samtio, R.H. Rajper, and A.S. Mastoi. Major Elements of Nari Formation Sandstone from Jungshahi Area of Southern Indus Basin, Pakistan. *Pakistan Journal of Scientific and Industrial Research Series A: Physical Sciences* 65(3): 248-259 (2022).
20. M.S. Samtio, A.A.A.D. Hakro, R.A. Lashari, A.S. Mastoi, R.H. Rajper, and M.H. Agheem. Depositional Environment of Nari Formation from Lal Bagh Section of Sehwan Area, Sindh Pakistan. *Sindh University Research Journal (Science Series)* 53(1): 67-76 (2021).
21. S.B. Ahmedani, A.A.A.D. Hakro, A.S. Mastoi, A.A. Halepoto, A.G. Sahito, S. Akhtar, and R.A. Lashari. Clastic Source and Depositional Environment of Mixed Carbonate-Clastic Sequences in the Oligocene Nari Formation from the Hundi Anticline, Karachi Embayment, Indus Basin, Pakistan. *Earth Sciences Research Journal* 29(2): 149-167 (2025).
22. A.M. Shar, A.A. Mahesar, G.R. Abbasi, A.A. Narejo, and A.A.A.D. Hakro. Influence of diagenetic features on petrophysical properties of fine-grained rocks of Oligocene strata in the Lower Indus Basin, Pakistan. *Open Geosciences* 13: 517-531 (2021).
23. A.M. Shar, A.A. Mahesar, A.A. Narejo, and N. Fatima. Petrography and Geochemical Characteristics of Nari Sandstone in Lower Indus Basin, Sindh, Pakistan. *Mehran University Research Journal of Engineering and Technology* 40(1): 82-92 (2021).
24. S.B. Ahmedani, M.H. Agheem, A.A.A.D. Hakro, A.A. Halepoto, R.A. Lashari, and G.M. Thebo. Integrated Petrographical, Mineralogical, and Geochemical Investigation to Evaluate Diagenesis of Sandstone: A Case Study of the Oligocene Nari Formation from Southern Kirthar Range, Pakistan. *Journal of Himalayan Earth Sciences* 57(1): 1-22 (2024).
25. F.K. Bender and H.A. Raza (Eds.). Geology of Pakistan. *Gebruder Borntraeger, Berlin, Germany* (1995).
26. A. Bilal, R. Yang, Y. Li, J. Zhang, H.T. Janjuhah. Microfacies shift in the Late Paleocene–Early Eocene Patala Formation in the Upper Indus Basin (Pakistan): Implications for development of the Ceno-Tethys Ocean. *Marine and Petroleum Geology* 161: 106693 (2024).
27. A.H. Kazmi and M.Q. Jan (Eds.). Geology and Tectonics of Pakistan. *Graphic Publishers, Karachi, Pakistan* (1997).
28. S.M.I. Shah (Ed.). Stratigraphy of Pakistan, Memoir 22. *Geological Survey of Pakistan, Quetta, Pakistan* (2009).
29. D. Bannert, A. Cheema, A. Ahmed, and U. Schaffer. The Structural Development of the Western Fold Belt, Pakistan. *Geologisches Jahrbuch Reihe* B80: 3-60 (1992).
30. R. Ahmed and J. Ahmed. Petroleum Geology and Prospects of Sukkur Rift Zone, Pakistan with Special Reference to Jaisalmer, Cambay and Bombay High Basins of India. *Pakistan Journal of Hydrocarbon*

Research 3(2): 33-41 (1991).
31. A.H. Kazmi and R.A. Rana. Tectonic Map of Pakistan. *Geological Survey of Pakistan Map Series, Quetta, Pakistan* (1982).
32. A.H. Kazmi and I.A. Abbasi. Stratigraphy and Historical Geology of Pakistan. *National Centre of Excellence in Geology, University of Peshawar, Pakistan* (2008).
33. A. Laghari, M.Q. Jan, M.A. Khan, M H. Agheem, A.G. Sahito, and S. Anjum. Petrography and major element chemistry of mafic dykes in the Nagar Parkar Igneous Complex, Tharparkar, Sindh. *Journal of Himalayan Earth Science* 46(1): 1-11 (2013).
34. M.Q. Jan, A. Laghari, M.A. Khan, M.H. Agheem, and T. Khan. Petrology of calc-alkaline/adakitic basement hosting A-type Neoproterozoic granites of the Malani igneous suite in Nagar Parkar, SE Sindh, Pakistan. *Arabian Journal of Geosciences* 11: 25 (2018).
35. S. Ahmed, S.H. Solangi, M.S.K. Jadoon, and A. Nazeer. Tectonic evolution of structures in Southern Sindh Monocline, Indus Basin, Pakistan formed in multi-extensional tectonic episodes of Indian Plate. *Geodesy and Geodynamics* 9(2): 358-366 (2018).
36. S.A. Abbasi, S.H. Solangi, and A. Ali. Seismic Data Interpretation: A Case Study from Southern Sindh Monocline, Lower Indus Basin, Pakistan. *Mehran University Research Journal of Engineering and Technology* 34(2): 107-115 (2015).
37. B. Wahid, S. ul Alam, A.S. Khan, A.A. Halepoto, and S. Jalal. Reservoir Characterization of Lower Goru Formation Using Seismic and Well Logs Data, Mubarak Gas Field, Lower Indus Basin, Pakistan. *Sindh University Research Journal (Science Series)* 55(2): 7-17 (2023).
38. M.A. Qureshi, S. Ghazi, M. Riaz, and S. Ahmad. Geo-seismic model for petroleum plays an assessment of the Zamzama area, Southern Indus Basin, Pakistan. *Journal of Petroleum Exploration and Production Technology* 11(1): 33-44 (2021).
39. R.D. Lawrence, R.S. Yeats, S.H. Khan, A. Farah, and K.A. DeJong. Thrust and strike slip fault interaction along the Chaman transform zone, Pakistan. *Geological Society, London, Special Publications* 9(1): 363-370 (1981).
40. A. Farah, G. Abbas, K.A. De Jong, and R.D. Lawrence. Evolution of the lithosphere in Pakistan. *Tectonophysics* 105(1-4): 207-227 (1984).
41. W.E. Crupa, S.D. Khan, J. Huang, A.S. Khan, and A. Kasi. Active tectonic deformation of the western Indian plate boundary: A case study from the Chaman Fault System. *Journal of Asian Earth Sciences* 147: 452-468 (2017).
42. Hunting Survey Corporation, Reconnaissance Geology of Part of West Pakistan. *A Colombo Plan Co-operative Project, Toronto, Canada* (1960).
43. A. Khan, M. Imran, M. Iqbal, and A. Nazeer. Structural Styles and Hydrocarbon Potential of Western Kirthar Fold Belt. *PAPG-SPE Annual Technical Conference(7^{th} - 9^{th} November 2011), Islamabad, Pakistan* (2011).
44. R.L. Folk and W.C. Ward. Brazos River Bar: A Study in the Significance of Grain Size Parameters. *Journal of Sedimentary Petrology* 27(1): 3-26 (1957).
45. A.A.A.D. Hakro, A.A. Halepoto, A.S. Mastoi, M.S. Samtio, R.H. Rajpar, and A. Noonari. Depositional Environment of Neogene Foreland Deposits (Manchar Formation) from the Bara Nai Section of the Southern Indus Basin, Pakistan. Pakistan Journal of Scientific and Industrial Research, Series A: Physical Sciences 68A(1): 96-105 (2025).
46. S.S. Jagirani, L. Bai, M.D. Jagirani, S.A. Panhwar, B. Neupane, K. Jagirani, W. Ghanghro, U. Baral, and Q.D. Khokhar. Sedimentological Study of Manchar Formation, Kari Buthi Section, Northern Laki Range, Southern Indus Basin, Pakistan. *International Research Journal of Earth Sciences* 8(2): 9-21 (2020).
47. W.C. Krumbein. Size frequency distributions of sediments. *Journal of sedimentary Research* 4(2): 65-77 (1934).
48. M. Khan, M.A. Khan, B.A. Shami, and M. Awais. Microfacies analysis and diagenetic fabric of the Lockhart Limestone exposed near Taxila, Margalla Hill Range, Punjab, Pakistan. *Arabian Journal of Geosciences* 11(2): (2018).
49. M. Rizwan, M. Hanif, N. Ali, and M. Ur Rehman. Microfacies analysis and depositional environments of the Upper Cretaceous Fort Munro Formation in the Rakhi Nala Section, Sulaiman range, Pakistan. *Carbonates and Evaporites* 35(4): (2020).
50. M. del C. Esqueda, E. Ríos-Jara, J.E. Michel-Morfín, and V. Landa-Jaime. The vertical distribution and abundance of gastropods and bivalves from rocky beaches of Cuastecomate Bay, Jalisco. México. *Revista de Biología Tropical*, 48(4): 765-775 (2000).
51. P. Zell, S. Beckmann, W. Stinnesbeck, and M. Götte. Mollusks of the upper Jurassic (upper Oxfordian-lower Kimmeridgian) shallow marine Minas Viejas formation, northeastern Mexico. *Journal of South American Earth Sciences* 62: 92-108 (2015).
52. A. Mancosu and J.H. Nebelsick. Echinoid

assemblages from the early Miocene of Funtanazza (Sardinia): A tool for reconstructing depositional environments along a shelf gradient. *Palaeogeography, Palaeoclimatology, Palaeoecology* 454: 139-160 (2016).
53. E.K. Yordanova and J. Hohenegger. Taphonomy of larger foraminifera: relationships between living individuals and empty tests on flat reef slopes (Sesoko Island, Japan). *Facies* 46: 169-203 (2002).
54. S.J. Beavington-Penney and A. Racey. Ecology of extant nummulitids and other larger benthic foraminifera: Applications in palaeoenvironmental analysis. *Earth-Science Reviews* 67(3-4): 219-265 (2004).
55. E. Özcan, A.O. Yücel, L.S. Erkızan, M.N. Gültekin, S. Kayğılı, and S. Yurtsever. Atlas of the Tethyan orthophragmines. *Mediterranean Geoscience Reviews* 4(1): 3-213 (2022).
56. A. Bilal, R. Yang, H. T. Janjuhah, M.S. Mughal, Y. Li, G. Kontakiotis, and N. Lenhardt. Microfacies analysis of the Palaeocene Lockhart limestone on the eastern margin of the Upper Indus Basin (Pakistan): Implications for the depositional environment and reservoir characteristics. *Depositional Record* 9(1): 152-173 (2023).
57. R.F. Gilham and C.S. Bristow. Facies architecture and geometry of a prograding carbonate ramp during the early stages of foreland basin evolution: lower Eocene sequences, Sierra del Cadí, SE Pyrenees, Spain. *Geological Society, London, Special Publications* 149(1): 181-203 (1998).
58. A. Abdullah, M. Mohibullah, A.K. Kasi, S. Ul Alam, and E. Ul Haq. Microfacies and Depositional Settings of the Eocene Nisai Formation, Pishin Belt, Pakistan. *Journal of Himalayan Earth Sciences* 56(1): 11-32 (2023).
59. U. Sarwar, S. Ghazi, S.H. Ali, M. Mehmood, M.J. Khan, A. Zaheer, and S.J. Arif. Sedimentological and sequence stratigraphic analysis of Late Eocene Kirthar Formation, Central Indus Basin, Pakistan, Eastern Tethys. *Earth Sciences Research Journal* 28(1): 29-38 (2024).
60. A.A.A.D. Hakro, W. Xiao, Z. Yan, and A.S. Mastoi. Provenance and tectonic setting of Early Eocene Sohnari Member of Laki Formation from southern Indus Basin of Pakistan. *Geological Journal* 53: 1854-1870 (2018).
61. G. Nichols (Ed.). Sedimentology and Stratigraphy. *Wiley-Blackwell, USA* (2009).
62. R.C. Selley (Ed.). Applied sedimentology. *Academic Press, London, UK* (2000).
63. S. Boggs (Ed.). Petrology of Sedimentary rocks. *Cambridge University Press, London, UK* (2009).
64. M. Lawal and M.H.A. Hassan. Sedimentary and stratigraphic characteristics of the Maastrichtian Dukamaje formation of southern Iullemmeden Basin: Implications for the paleogeography of the Upper Cretaceous trans-Saharan seaway. *Journal of African Earth Sciences* 200: 104878 (2023).
65. J.L. Melvin (Ed.) Evaporites, Petroleum and Mineral Resources. *Elsevier* (1991).
66. S.F. Könitzer, S.J. Davies, M.H. Stephenson, and M.J. Leng. Depositional controls on mudstone lithofacies in a basinal setting: implications for the delivery of sedimentary organic matter. *Journal of Sedimentary Research* 84(3): 198-214 (2014).
67. H.B. Stewart. Sedimentary Reflections of Depositional Environment in San Miguel Lagoon, Baja California, Mexico. *Bulletin of the American Association of Petroleum Geologists* 42(1): 2587-2618 (1958).
68. R. Passega. Grain size representation by CM patterns as a geologic tool. *Journal of Sedimentary Research* 34(4): 830-847 (1964).
69. B.K. Sahu. Depositional Mechanisms from the Size Analysis of Clastic Sediments. *Journal of Sedimentary Research* 34(1): 73-83 (1964).
70. S.K. Ghosh and B.K. Chatterjee. Depositional mechanisms as revealed from grain-size measures of the palaeoproterozoic kolhan siliciclastics, Keonjhar District, Orissa, India. *Sedimentary Geology* 89(3-4): 181-196 (1994).